Lowland Technology International 2017; 19 (3): 151-164
International Association of Lowland Technology (IALT): ISSN 1344-9656
Special Issue on: Kumamoto Earthquake & Disaster

Research Paper

Analysis of a Fast-Moving Landslide during an Earthquake in Japan

K. Ishihara

ARTICLE INFORMATION

Article history:

Received: 06 March, 2017
Received in revised form: 26 November, 2017
Accepted: 29 November, 2017
Publish on: 08 December, 2017

Keywords:

Landslide
Earthquake
Constant-volume triaxial test
Residual strength
Water content

ABSTRACT

In an effort to determine the residual strength from the laboratory tests, a new type of tests termed “constant-volume triaxial test” was performed on non-saturated specimens of silty sand prepared at varying water contents. The results of the tests disclosed that the water content or saturation ratio is a key parameter governing the residual strength of the non-saturated soil tested in the above manner. Back-analysis was also made to determine the residual strength that might have been mobilized in the landslide triggered at Tsukidate at the time of the May 26, 2003 earthquake. The comparison of these two data showed a reasonable degree of coincidence, indicating that the proposed method of the laboratory triaxial tests would be a promising means for estimating the residual strength of given soils.

1. Introduction

Problems associated with landsliding would be two-fold, namely, to assess whether a given slope will slide or not by some external agencies such as rain-falls and earthquakes, and secondly to estimate how far downhill the sliding mass of soils or rocks will travel. The issue of triggering has been discussed extensively by professionals in the disciplines of geology geomorphology and geotechnology. The issue of the post-failure travel distance has also been the subject of concern for many researchers and numerous attempts have been made to clarify mechanism of debris flow based on case studies and analyses. A comprehensive overview and summary on the out-comes of these studies in recent times is given in a paper by Hunter and Fell (2003). It appears, how-ever, that the approach from the viewpoint of material behaviour has not often been explored and the problems remain untouched particularly for soil materials which are not fully saturated. In view of the fact that a majority of soils and rocks involved in landslides are not necessarily saturated fully with water, it was felt necessary to explore a possibility of identifying behaviour of partly saturated soils based on the laboratory tests. This is an incentive to initiate the study described in this paper.

At the time of the Miyagiken-Oki earthquake of May 26, 2003, a landslide occurred on a gentle slope with a velocity on the order of 3-6m/sec. The rapid movement of the sliding soil mass resulted in the spreading of the debris in the flat land downhill. In order to provide some data on soil strength that is mobilized during this type of flow failure, several series of laboratory tests were performed by using the triaxial test apparatus on silty sands secured from the landslide site. The results of initial phase of the tests are described in this paper.

On the other hand, by postulating a simple kinematic model for the sliding and spreading of soil debris, the

Professor Research and Development Initiative, Chuo University, Tokyo 192-0393, JAPAN, kenji-ishihara@e-mail.jp
Note: Discussion on this paper is open until June 2018.

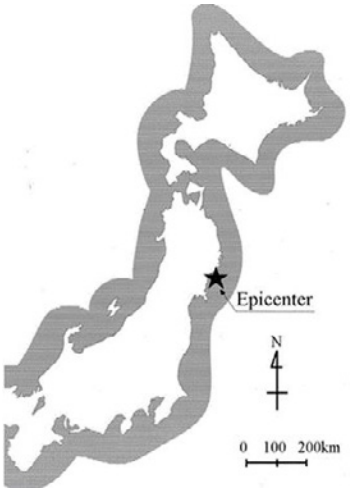

Fig. 1. Epicenter of the May 26, 2003.

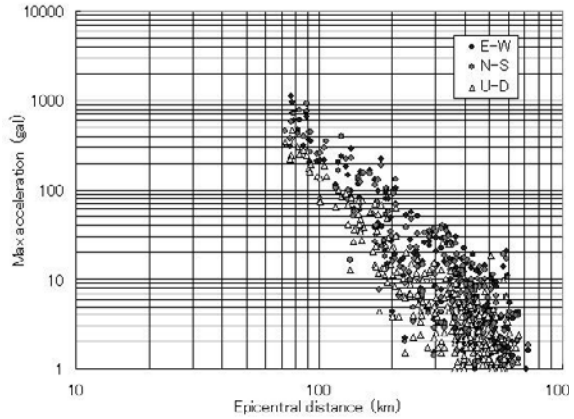

Fig. 2. Recorded peak horizontal accelerations plotted versus the epicentral distance ground.

residual strength was back-estimated for the case of the above-mentioned landslide. The outline and some results of the back-analysis will also be presented in the following pages of this paper.

2. Miyagiken-Oki Earthquake, May 26, 2003

A large earthquake rocked the eastern part of Miyagi Prefecture at 18:24 on May 26, 2003 with a magnitude of M = 7.0 (Yasuda et al. 2004). The epicenter was located about 30km off the coast of the city of Sendai, as shown in **Fig. 1** and its focal depth was 71km. Major damage was collapse or injury to local houses, crest settlements or cracks to river dikes, ground movements in port and harbour areas due to liquefaction, and a landslide which occurred at Tsukidate about 40km inland from the coast. A number of strong motion recorders were triggered and monitored the shaking during the earthquake. The peak horizontal accelerations recorded are plotted in **Fig. 2** against the epicentral distance where it is noted that there

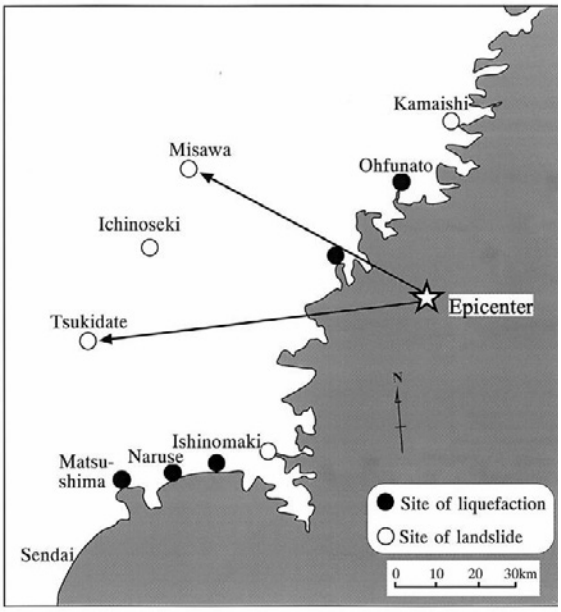

Fig. 3. Location of the landslide at Tsukidate.

is no data within short distances as it was an offshore event.

The peak horizontal acceleration at Mizusawa which is the nearest from the site of landslide was 360gal. Thus, the landslide is considered to have been triggered by this strong shaking in the gentle slope at Tsukidate whose exact location is shown in **Fig. 3.** The aerial views of the landslide are shown in **Fig. 4** and the plan view is displayed in **Fig. 5** where it can be seen that the portion of the slope about 40m wide and 80m long moved downhill and spread out over the paddy fields downhill covering an area about 50m wide and 100m long.

The place of the slide had been a small valley-shaped depressed land, but about 40 years ago it was filled by silty sands from nearby borrow site in order to provide flat farmlands over the slope. The longitudinal cross section of the stripped-off portion is shown in **Fig. 6.** The soils involved in the slide are of volcanic tuff and pumice origin and the fill was in a very loose state without any compaction. About 200m uphill the headwall scars there is a gently sloped ridge of the hill running in the direction perpendicular to the slide line and there is no source of constant water supply which can be identified from the surface survey. Over the exposed sliding surface, a few springs were discovered, however, and the water was stored in a small pond near the lower portion of the slide, providing water supply for irrigation of the rice field downhill. Thus, though not in a large quantity, the water from occasional rainfalls must have accumulated in the buried valley, thereby raising the level of the ground water table particularly in the area of the landslide. It is reported that the ground water table was located about 3-5m below

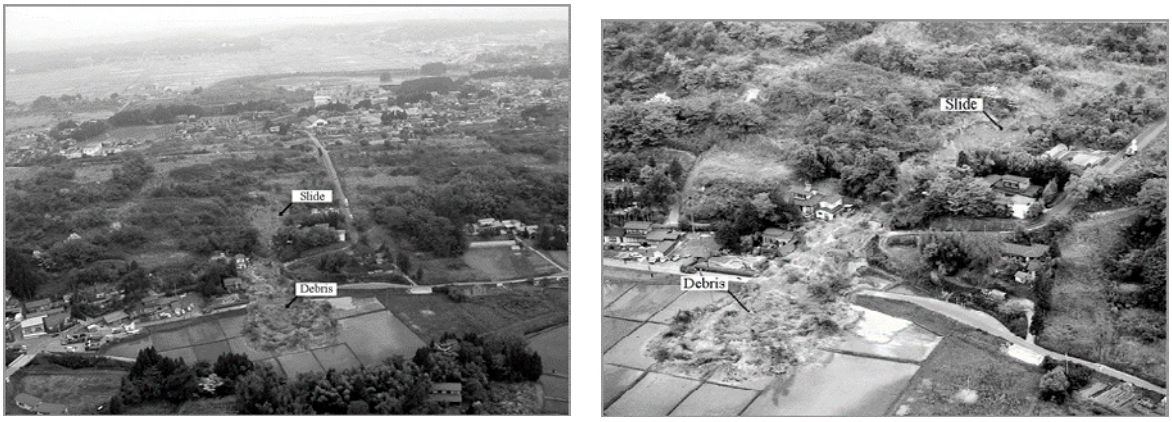

Fig. 4. Aerial views of the Tsukidate landslide.

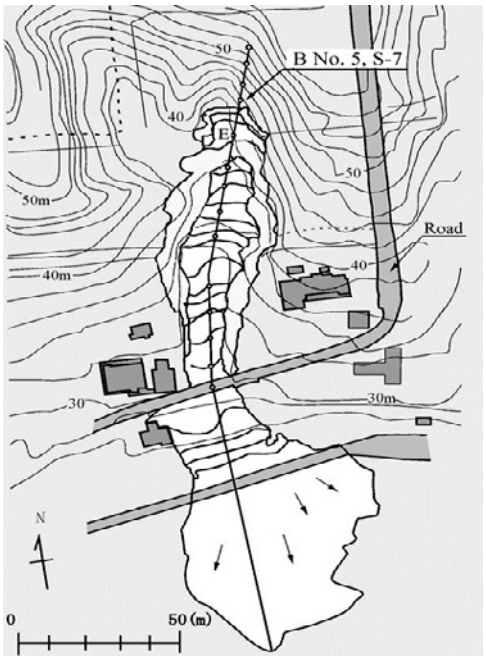

Fig. 5. Plan view of the landslide area at Tsukidate.

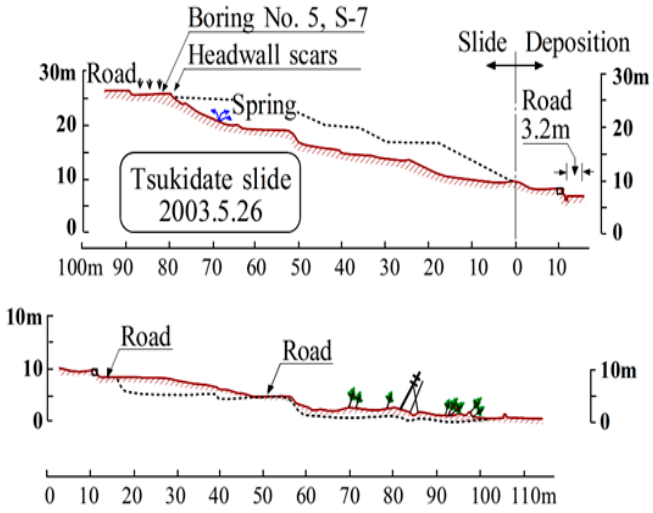

Fig. 6. Longitudinal cross section after the slide

the surface, making the volcanic ash soil saturated in a loose state. It is believed highly likely that liquefaction had developed around the depth of slip plane by the strong enough shaking during the earthquake and this led to the complete failure of the slope.

The soil from volcanic origin typically has a grain size distribution curve as shown in **Fig. 7** with fines of about 40%. According to the report of Japanese Geotechnical Society (JGS), the water content of soils sampled at several locations showed values of w = 25~60% and void ratio ranged between 0.910 and 1.175. Specific gravity was 2.313 to 2.478. The saturation ratio was between 60 and 100%. Each particle contains inside voids, making the particle itself easily crushable. Thus, the nominally measured value of void ratio is considered smaller than that of the actual void ratio. Undisturbed samples were secured from the exposed surface of the slide and tested in the laboratory. The results of the cyclic triaxial tests on undisturbed samples conducted by Soil Mechanics Laboratory of Chuo University showed that the cyclic strength defined as the cyclic stress ratio causing 5% double amplitude axial strain is as low as 0.19 for the 20 cycles of uniform load application. Such a low resistance seems to provide an evidence for triggering liquefaction under the given cyclic shear stress as represented by the ground surface acceleration on the order of 360gal.

Several in-situ sounding tests were performed after the earthquake by means of the Standard penetration test and also by Swedish Cone Penetration technique. One of the test results at a place a few meters uphill the head scarp **(Figs. 5, 6)** is demonstrated in **Fig. 8.** It may be speculated that the near-surface volcanic soil deposit with a low SPT

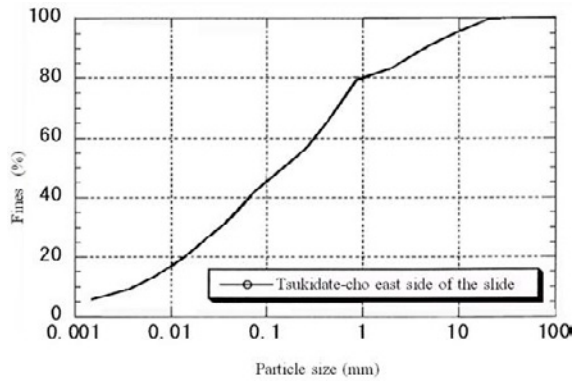

Fig. 7. Grain size distribution curve of a representative soil from Tsukidate landslide site.

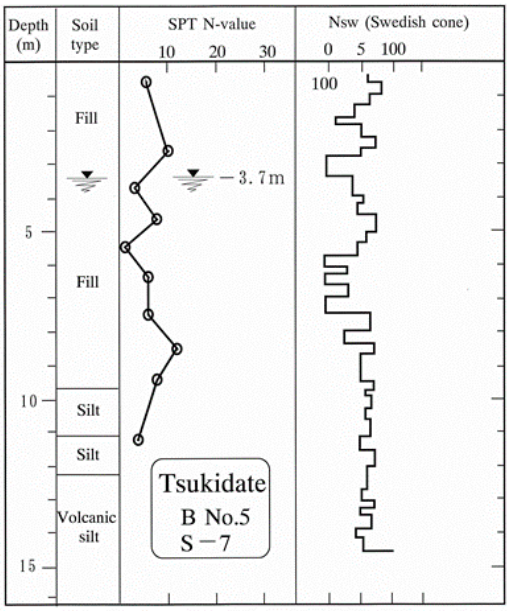

Fig. 8. Soil profile and penetration resistance at a place about 2m uphill from the headwall scarp (after JGS report).

blow count values of N=1-5 and a static Swedish cone-penetration resistance of N_{sw} = 0~50kN had been in a state of loose deposition vulnerable to liquefaction.

Apart from the triggering mechanism, another issue of importance would be the distance through which the debris did travel downhill. To investigate this aspect, some laboratory tests were conducted along with a simple analysis to back-estimate the residual strength of the volcanic soil which is mobilized at a largely deformed state. The outcome of these studies will be described in the following pages of this paper.

3. Volume change-controlled triaxial test

3.1 Basic Concept

Downslope movement of soil or rock masses at a fast speed is considered frequently to take place when landslides occur in steep slopes or they are triggered by strong shaking during earthquakes. In any event, it may be taken for granted that, when the materials are fully saturated, the movement of the debris takes place under undrained conditions, that is, without any volume change whatsoever. When the sliding soils or rocks are partially saturated which are generally the case, the volume of the sliding debris may increase or decrease. However, there would be little time for the soils or rocks to change its volume in the rapid movement and consequently, it may as well be assumed that the sliding would take place under the condition of practically no volume change. It would appear likely that, when the materials start to move, immediately following the slide, they are once bounced and put into a loose state to facilitate the subsequent sliding. Thus, in the course of sliding, the soils or rocks are considered in a contractive state, having a potential to decrease their volume if it is allowed in fact to occur. However, because of the rapidity in the speed of movement, there would be little time for soil mass to reduce its volume and, it may be roughly assumed that the shear deformation takes place under a constant volume condition even when the material is not fully saturated. In order for the potentially contractive material to keep its volume unchanged during shear, the confining stress due to the overburden acting initially on the soil or rock skeleton must be reduced via unloading. However, the initial overburden pressure has to remain unchanged all the way through the sliding process including the initial state before the outset of the landslide. Thus, the portion of the initial confining stress reduced by the unloading must be carried by other substances existing in the pores of the sliding materials. In the case of saturated materials, the water in the pores could play this role, because of its extremely low compressibility as compared to that of the soil skeleton. If the pores are filled with compressible materials such as air-containing water or dust-containing air, the contraction of soil skeleton must occur if the loading is sufficiently slow. However, when the load application is rapid enough, even the compressible substances in the pores might temporarily carry the load due to the delayed nature of the volume change or contraction of the skeleton of the soils or rocks which will continue during the entire process of rapid landsliding. This could be the case because the speed of shear deformation would by far transcend the speed of volume contraction. Thus, it will be assumed in the pre-sent study that the volume of even partly saturated soils be maintained almost unchanged during the application of shear stress. The laboratory tests simulating the above

scenario were then attempted and the following is the description on the conduct of the tests and their results.

3.2 Triaxial test apparatus

The large triaxial test apparatus equipped with an inner cell was used in the present study. As shown in **Fig. 9,** this apparatus can accommodate cylindrical triaxial soil specimens of 12.0 cm in diameter and 24.0 cm in height. The inner cell was newly installed within the triaxial cell, in order to measure volume changes of non-saturated soil specimens during drained or undrained loading. In the test, the triaxial cell was submerged to the level of a small-diameter mouth of the inner cell as indicated in **Fig. 9,** whereby leaving compressed air in the upper portion of the cell. When the unsaturated soil specimen causes volume change, the water level located at the narrow mouth of the inner cell changed accordingly. The change in the water level was then monitored by means of a minute differential pressure transducer, which is connected to the inner cell and by the burette outside the cell, as shown in **Fig. 9.**

As the inner cell is subjected to the identical pressure both from inside and outside, there is no lateral deformation in the inner cell itself. Therefore, the volume change of the specimen can be calculated as the change in the water level multiplied by the area of the cross section of the narrow mouth of the inner cell.

3.3 Test procedures adopted

In order to implement the volume-constant condition for non-saturated samples in the triaxial compression test, it is necessary to appropriately control the axial stress and cell pressure as well. The control of the stresses may be done in various manners, but after several searches by trial and error, the following scheme was considered most appropriate and adopted in the tests of the present study. This test scheme will be referred to, as “constant volume drained test” is as described below.

(1) After preparing non-saturated samples in the triaxial cell, a confining stress is applied to produce a state of consolidation.

(2) Then, the axial strain is given to the sample with a specified constant rate. During this phase of strain application, the axial stress is monitored by a load cell along with the volume change of the sample.

(3) Since the sample starts to increase its volume from the beginning, then it is necessary to reduce the cell pressure to keep the volume unchanged while continuing the axial strain application at the given rate.

(4) The reduction in the cell pressure is continued until its value become equal to zero. Even after that, the application of the axial strain is continued with zero cell pressure until an axial strain of about 10% is attained.

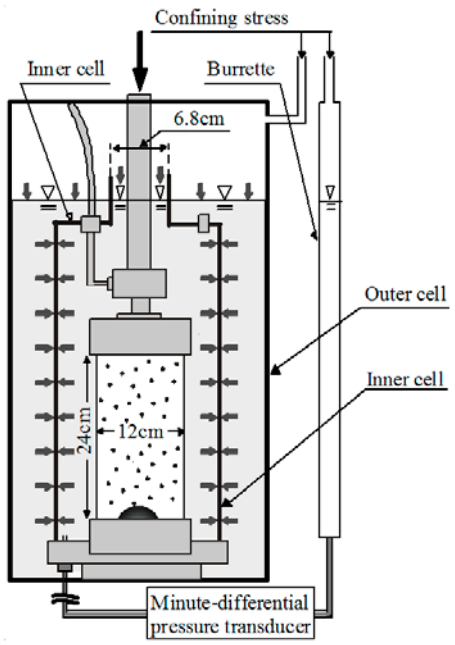

Fig. 9. Triaxial test apparatus with an inner cell.

To illustrate the conduct of the tests following on the above procedures, two fully saturated samples of Toyoura sand were prepared to have a relative density of Dr = 30% and consolidated isotropically to a confining stress of $\sigma'_{1c} = \sigma'_{3c}$ = 98kPa. One sample was tested under undrained condition in a conventional manner by applying a constant rate of axial strain of 0.24% per minute. Another sample was tested under drained condition, while applying the same speed of axial strain, that is, ε_1 = 0.3% per minute, and by following the same test procedures from (1) to (4) described above.

The results of such two tests are shown together in **Fig. 10** in terms of the monitored key parameters plotted versus time. **Fig. 10(a)** shows the axial strain, ε_1, at the constant speed plotted versus time. Note that the axial strain application is the same for both of the undrained and drained tests. The controlled change in the cell pressure σ_3 are shown in **Fig. 10(b)** versus time where it is noted that the value of σ_3 remained unchanged in the undrained test. In the case of the drained test, it is seen that the cell pressure was decreased relatively fast within 30 seconds at the beginning but somewhat slowly near the end until it became equal to zero at 700 seconds after the start of the test. A kink at 400 seconds does not mean anything special, but a mere consequence resulting from the control of the cell pressure so as to keep the volume of the sample unchanged. The monitored value of the axial stress σ_1 is shown in **Fig. 10(c)** versus time where it may be seen that the axial stress reached an almost constant value at 700 seconds as well and stayed there all the way afterwards. On the basis of the axial and cell pressures as measured

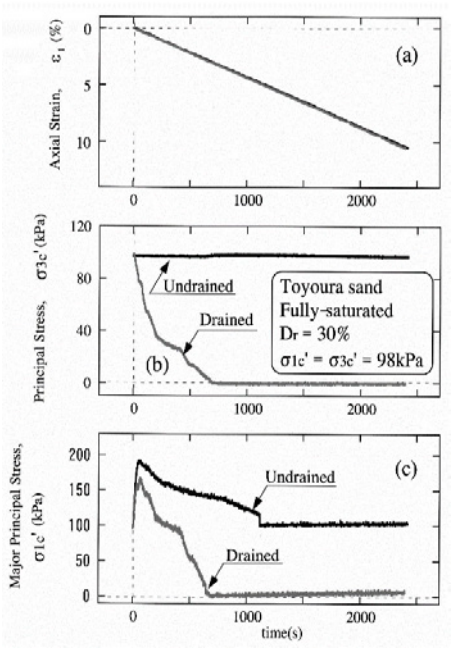

Fig. 10. Time-change in axial and confining stresses and axial strain in the constant-volume tests on saturated Toyoura sand.

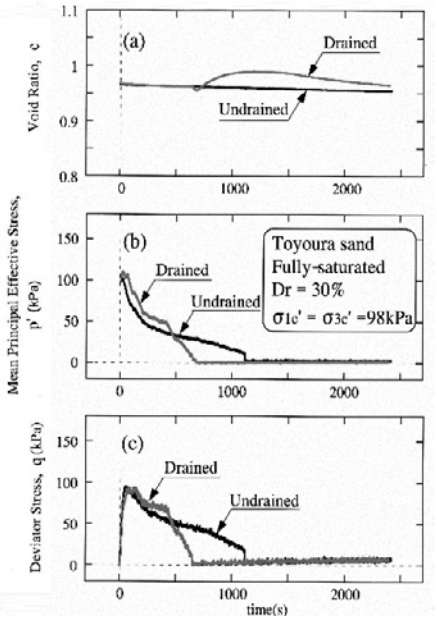

Fig. 11. Time-change in void ratio, p' and q in the constant volume tests on saturated Toyoura sand.

above, the deviator stress $q = \sigma_1-\sigma_3$ and the mean principal stress $p = (\sigma_1+2\sigma_3)/3$ are calculated and shown plotted versus time in **Figs. 11(a) and 11(b).** It may be seen that, in both of the un-drained and drained tests, the value of q is observed increasing first and decreasing after it reached a peak value. The value of p is seen always decreasing. The timewise variations of void ratio are shown in **Fig. 11(c),** where it is noted that, while the void ratio stayed unchanged until 700 seconds, it tended to increase slightly afterwards in the drained test. The test results as presented above are alternatively shown in **Fig. 12** in the form of four figures in one set, that is p-q stress path, q-ε_1 stress-strain diagram, void ratio versus p curve, and the void ratio versus axial strain diagram.

The plots in **Fig. 12** appear to indicate that, the undrained behaviour of saturated Toyoura sand is reproduced, to a reasonable level of accuracy, in the saturated sample's behaviour that was obtained in the volume change-controlled manner under drained condition. It is to be noticed that the coincidence is reasonably satisfactory when attention is drawn particularly to the largely deformed state of the sample where the residual strength is attained. In **Fig. 11(c),** it was noted that the void ratio tends to increase slightly at the end of the drained test. In performing the test, it was difficult to control the cell pressure at this stage so as to keep the void ratio unchanged while holding the stress ratio, q/p, at a sufficiently large critical value corresponding to failure.

This may be an issue to be resolved in future by introducing a more refined set of measuring and control system. It is not known, however, whether the increase of void ratio at large strains could occur as a result imperfection in monitoring or control system or as a consequence of incapability of inherent response of sand. In any event, without pursuing this feature, the test procedures as monitored above were adopted in the recent study in conducting other series of tests on silty sands to determine the residual strength.

3.4 Test material

The silty sand tested was secured from the site of Tsukidate landslide which occurred at the time of the Miyagiken-Oki earthquake of May 26, 2003 in Japan. The original soils as recovered at the site was sieved into materials with different grain sizes and they were blended to obtain a test material which is considered representative of the in-situ soils in term of grading. The grain size distribution curve of the soil thus obtained is shown in **Fig. 13.** It is noted that it contains 36% of fines and has a specific gravity of $G_0 = 0.264$ and mean diameter $D_{50} = 0.252$mm.

3.5 Results of the constant-volumes tests

The first series of the tests was intended to clarify effects of density on the residual strength of the silty sand from Tsukidate landslide site. Three specimens with the relative density of $D_r = 72$, 76 and 83% after consolidation were tested with the results shown in **Fig. 14** where the axial strain ε_1, confining stress σ3 and axial stress σ1 are

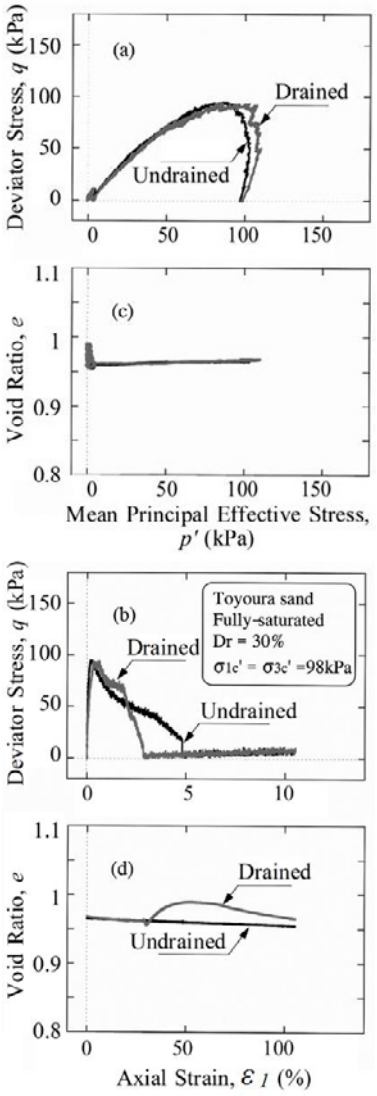

Fig. 12. Stress path, stress-strain, e-p' and e-ε1 diagrams in the constant volume tests on saturated Toyoura sand.

plotted versus time. Note that the relative density as the sample was prepared was D_r = 5, 10 and 30%, respectively. However, after consolidation the relative density increased pronouncedly because of high fines content. It is noted that the cell pressure σ_3 was reduced to zero at 700 seconds after the start of the test where the axial stress because equal to σ_3 = 50kPa. These basic data are alternatively demonstrated in **Fig. 15** where the void ratio, mean principal stress and deviator stress are shown plotted against time. It is noted that within the range of initial relative density variation of D_r = 5~10%, or within the range of post-consolidation relative density of D_r = 72~83% there is practically little difference in the residual strength when the soil is deformed largely. The same results of the three tests are presented in **Fig. 16** in a set of four diagrams, where it may be seen that there are some dilation of the specimens at axial strains in excess of ε_1 = 3%. The stress path and stress-strain relations show

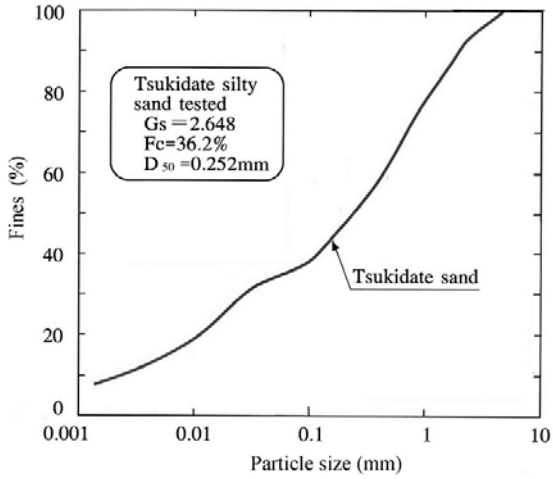

Fig. 13. Grain size distribution curve of a soil sample used for the tests.

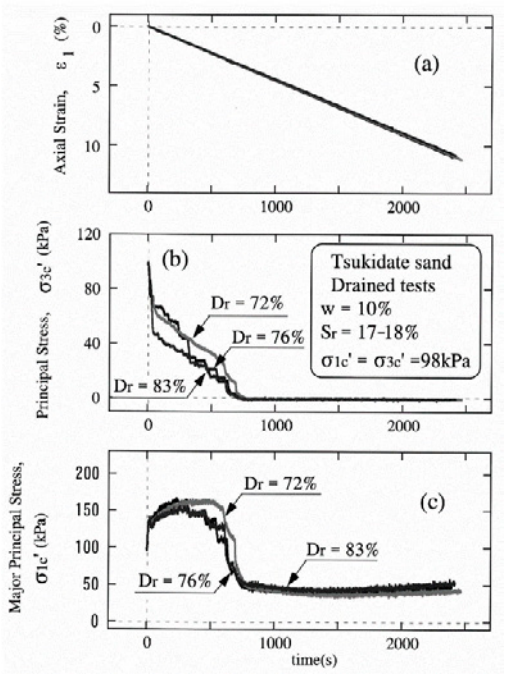

Fig. 14. Time change in ε_1, σ_1 and σ_3 in the constant volume tests on Tsukidate silty sand with different relative densities.

almost similar but slightly different shape in the early stage of strain application, but practically the same deviator stress q in the later stage when the specimens were deformed largely. It may thus be mentioned that the residual strength is determined uniquely irrespective of the density in the range of D_r = 72 and 80% after the consolidation. It is to be remembered that the relative density nominally determined tends to stay within a narrow range, if the soil consolidation pressure is as large as 98kPa. Thus, in such conditions the effect of density becomes less pronounced.

The second series of the tests was carried out to see effects of the initial consolidation pressure. In the three

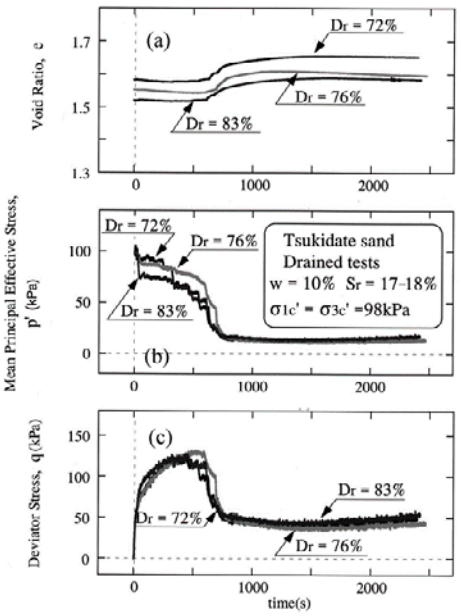

Fig. 15. Time change in e, p' and q in the constant volume tests on Tsukidate silty sand.

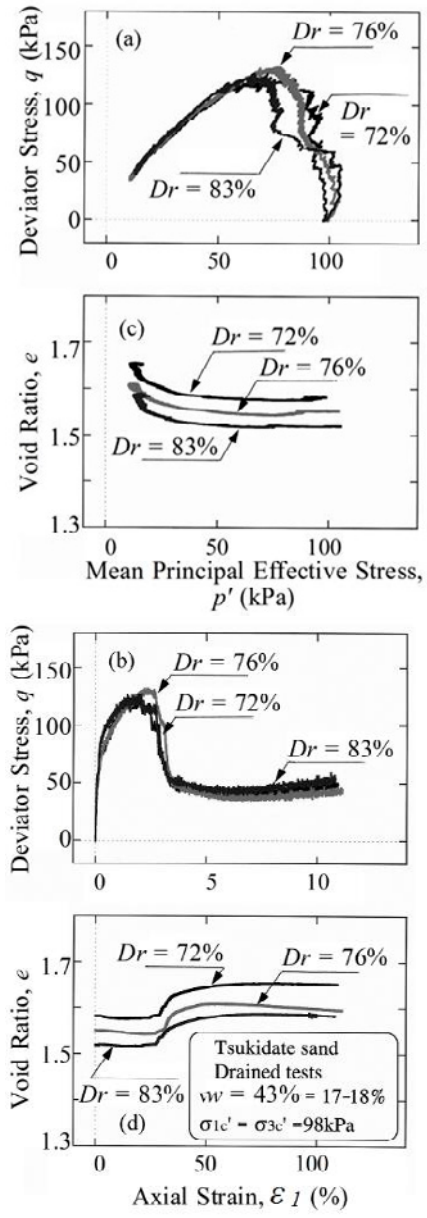

Fig. 16. Stress path, stress-strain, e-p' and e-ε_1 diagrams in the constant volume tests on saturated Toyoura sand.

tests, the initial confining stress was changed as σ'3c=49, 98 and 196kPa. The three samples had a relative density of D_r = 72~93% after consolidation. Because of the silty sand containing 36% of fines, the relative density became larger as the consolidation pressure increased. The raw test data are presented in **Fig. 17** in terms of each monitored value plotted versus time. It is seen apparently that the sample with higher density exhibits higher peak deviator stress and correspondingly larger dilatancy at the later stage of strain application. The test data were arranged otherwise as presented in **Fig. 18,** so that time wise variation of p, q and e are visible. It is worthy of notice that the deviator stress q converges to an identical value irrespective of the initial confining stress and thus leads to a unique value of the residual strength. The test data as above were re-arranged in **Fig. 19** in the form of four diagrams where it can be seen that despite the difference in size of each curve, the shape is similar converging to a constant value of the deviator stress. The above observation may lead to the conclusion that the residual strength mobilized at largely deformed stage of the sample can be determined uniquely irrespective of the initial confining stress σ'_{3c} .

The third series of the tests was conducted to see the effects of water content, w, or saturation ratio, Sr. The tests were performed on specimens consolidated to an effective confining stress of σ'_{3c} = 98kPa having the relative density after consolidation in the range of D_r = 78~85%. Three tests were performed on specimens having different water content of w = 20, 43 and 48%. The raw test data are presented in **Fig. 20** with the parameters ε_1, σ_1 and σ_3 plotted against time. **Fig. 21** shows the same test data demonstrated in the form of time-change of p, q and e. The set of four diagrams is demonstrated in **Fig. 22** where it can be seen that the residual strength of Tsukidate silty sand mobilized at the largely de formed state tends to decrease with increasing water content, particularly in the range of large water content in excess of about 20%. The residual strength defined as half of the deviator stress qs at large strains is read off from the test data in **Fig. 22** and plotted versus water content and saturation ratio in **Fig. 23.** It can be seen that the residual strength takes a nearly constant value of 23kPa up to the water content of about 20% but it starts to decrease sharply with increasing water content down to S_u=5kPa or even lower when the saturation ratio be-comes more than 85%.

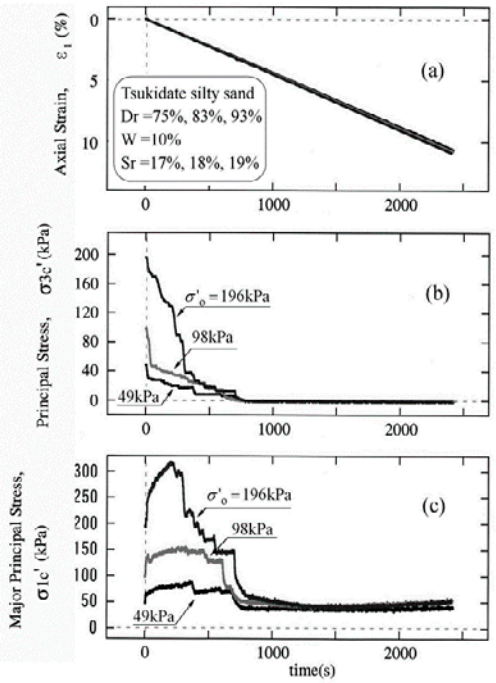

Fig. 17. Time change in axial and confining stresses, and axial strain in the constant-volume tests on Tsukidate silty sand

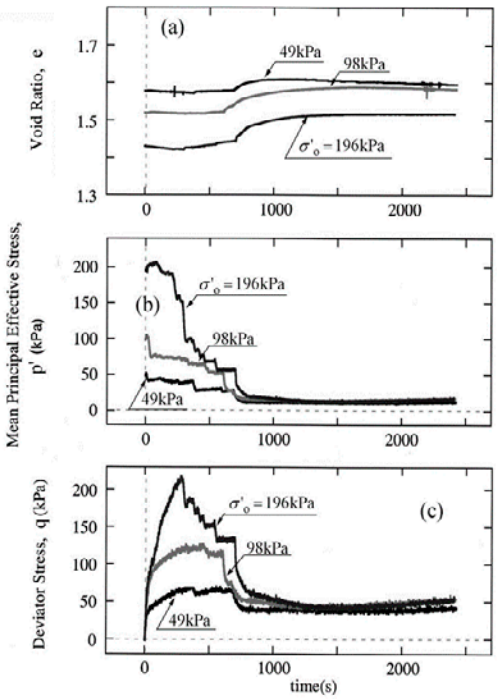

Fig. 18. Time change void ratio, p' and q in the constant volume tests on Tsukidate silty sand.

4. Kinematic model for back-analysis

The level of hazard caused by a landslide is governed by the distance through which debris will travel downhill after the slide has been triggered. If the debris flows over substantial distances, potential damage to property and human life becomes extensive. For the estimate of a runout distance of the debris, the residual strength of a flowing mass is deemed to play a pivotal role. Thus, while its estimate by laboratory tests is useful, the efforts to explore the magnitude of residual strength from back-analyses of what has actually happened would be by far an important aspect. In order to fulfill this task, some kinematic models have to be assumed which are simple, yet could capture the essence of the phenomenon. This type of problems was discussed by Jayapalan (1983) in relation to the breach of mine waste disposal ponds.

The model descried below is the one proposed by Hungr (1995) and would be one of the simplest ways for duplicating a sequence of events during landsliding.

Let the soil mass in a slope be considered to slide down the slope and come to standstill as shown in **Fig. 24.** This process may be divided into two parts, namely, (1) the block sliding on the slope without changing its original configuration and (2) the spreading over flat or gently sloped ground, as illustrated in **Fig. 24.** In the course of the block sliding, the movement of soil or rock mass may be assumed to be resisted along its base by the frictional force as illustrated in **Fig. 25(a).** Thus, the strength during sliding is given by

$$S'_u = \mu \gamma_t H_o \cos\alpha \qquad [1]$$

Where μ is the friction coefficient, γ_t denotes unit weight of soils or rocks, α is the slope angle and H_0 donotes the thickness of the sliding mass.

In next stage in which spreading occurs, the resistance is also mobilized at the base, which may be taken as equal to the residual strength S_u. Postulating the shape of the debris surface to be roughly represented by a parabolic curve, the equation to estimate the residual strength is given as

$$S_u = \gamma_t H_o^2 x_o / 4(x_f^2 - x_o^2) \times \left(8 - 9\, x_o / x_f\right) \qquad [2]$$

Where x_0 denotes width of the sliding mass. In deriving this equation, the energy loss due to the frictional resistance at the base is assumed to be equal to the gain in energy due to the lowering of the center of gravity which is denoted by Δh in **Fig. 25(b).**

This assumption may not be correct, because significant deformation takes place in the interior of the spreading materials and some amount of energy should be consumed in the process of deformation in addition to

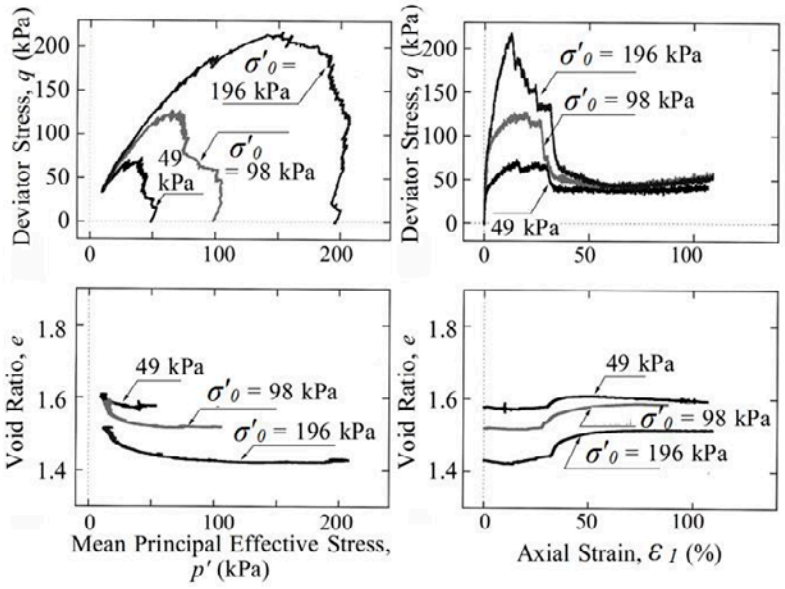

Fig. 19. Stress path, stress-strain, e-p' and e-ε_1 diagrams in the constant volume tests on Tsukidate silty sand.

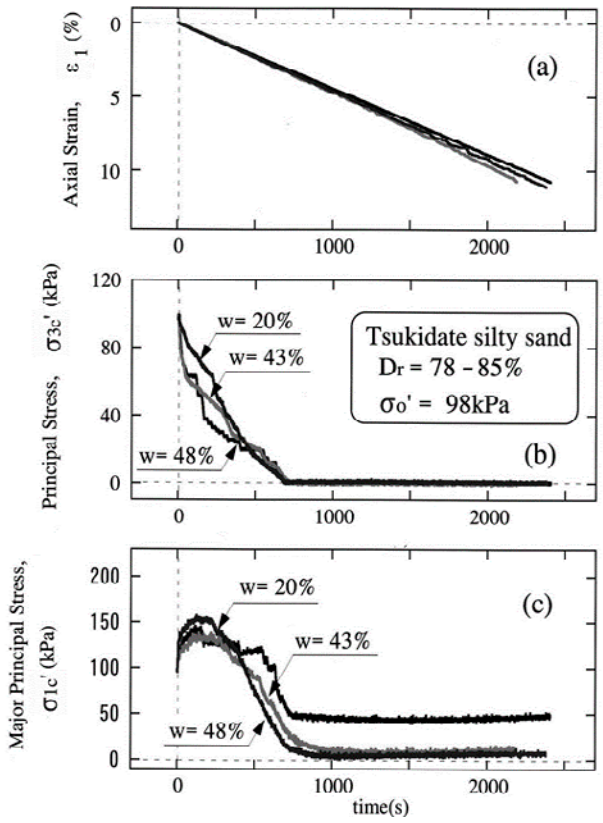

Fig. 20. Time change in axial and confining stresses, and axial strain in the constant-volume tests on Tsukidate silty sand.

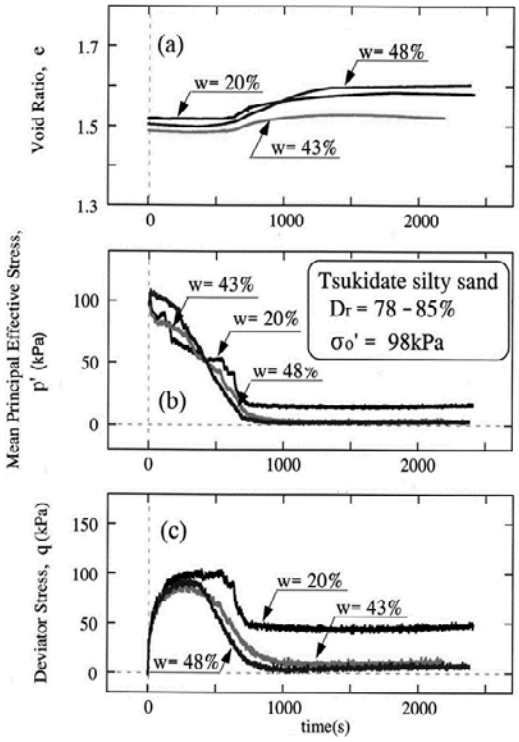

Fig. 21. Time change void ratio, p' and q in the constant volume tests on Tsukidate silty sand.

the energy spent at the base of the spreading mass. Therefore, the value of S_u back-calculated by Eq. (2) would overestimate the actual residual strength. In the following, the value of Su estimated by Eq. (2) will thus be taken as the maximum possible value of S_u.

In actual cases of landsliding, the above two phases of mass movement and deformation may take place in succession, and more complicated computation becomes necessary. The derivation of the equation for somewhat complicated cases can be done as follows with reference to the notations shown in **Fig. 26.**

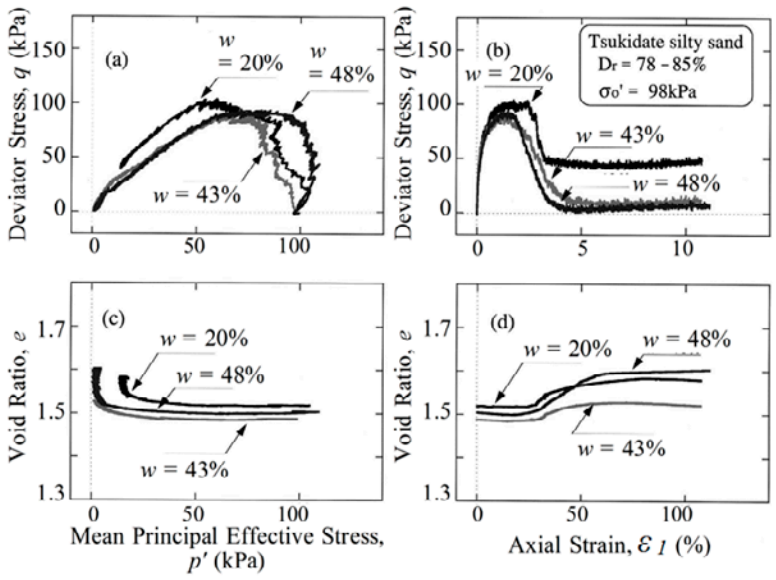

Fig. 22. Stress path, stress-strain, e-p' and e-ε1 diagrams in the constant volume tests on Tsukidate sites sand.

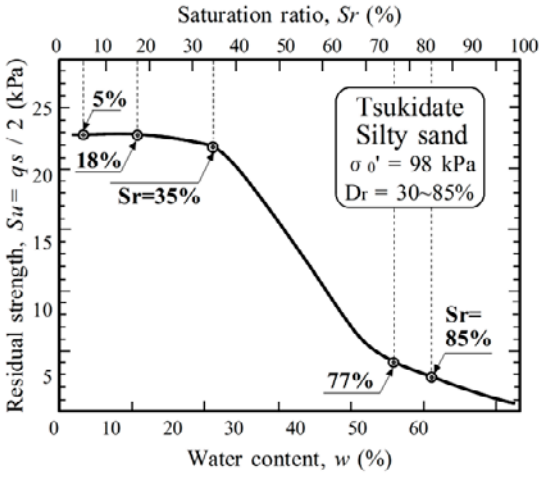

Fig. 23. Residual strength versus water content.

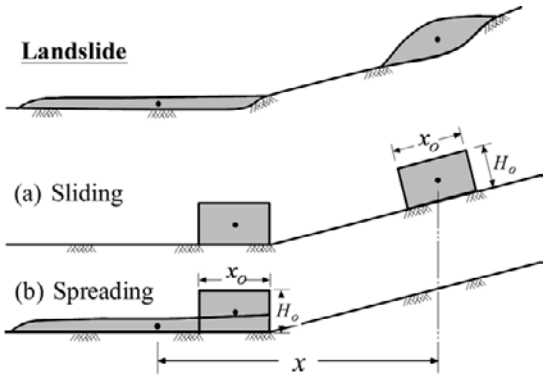

Fig. 24. A landslide model consisting of sliding and spreading.

4.1 Equality of volume

Assuming the parabolic configuration after the spreading, the volume of the spread-out mass is given by $2H_f x_f/3$. Thus, the conservation of the volume is expressed as

$$H_o x_o = \frac{2}{3} H_f x_f \qquad [3]$$

4.2 Energy gain due to slide-down of the mass

From the geometrical consideration, the lowering of the center of gravity height Δh is given by

$$\Delta h = \frac{H_o}{2}\cos\alpha - \frac{3}{8}H_f + h - \frac{x_o}{2}\sin\alpha \qquad [4]$$

Thus, the gain in energy, ΔE, in height is given as

$$\Delta E = \gamma_t H_o x_o \Delta h \qquad [5]$$

4.3 Loss of energy, ΔW

Due to the resistance at the base of the sliding mass in the slope and at the bottom of the spreading mass, the energy loss is given by

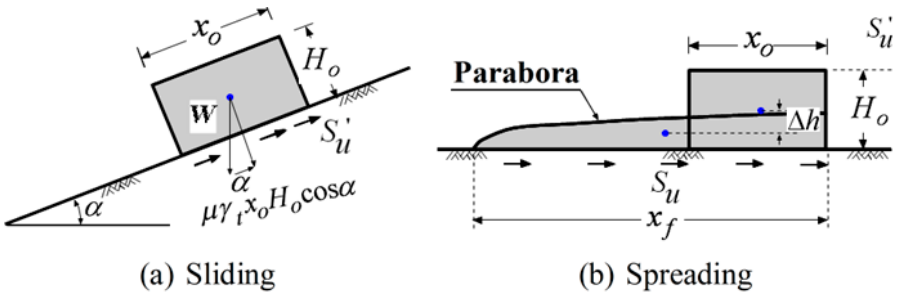

Fig. 25. Two phases of landsliding.

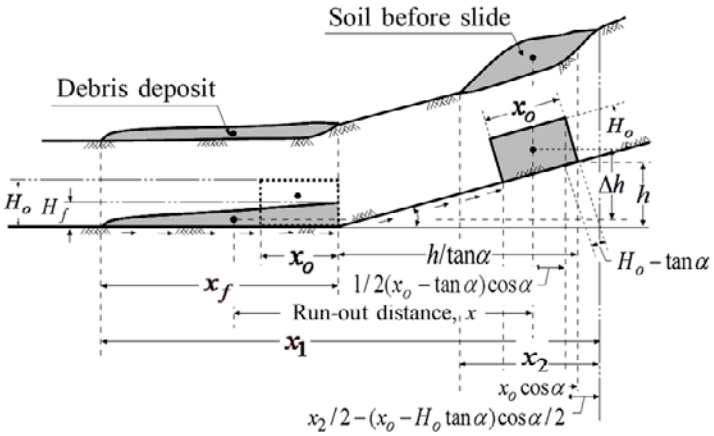

Fig. 26. A kinematic model for landsliding.

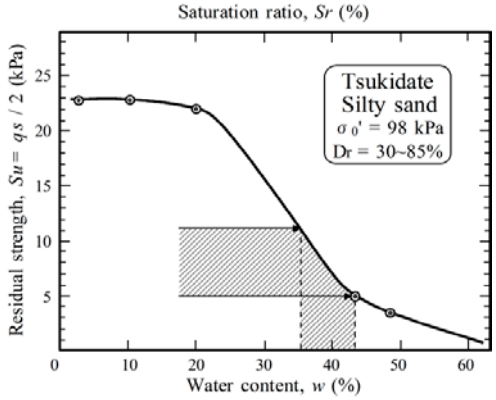

Fig. 27. Comparison between back-estimated and the laboratory-determined value of the residual strength.

$$\Delta W = \int_{x_o}^{x_f} \frac{S_u x}{2} dx + \mu\gamma_t H_o x_o \cos\alpha \frac{h}{\sin\alpha} \quad [6]$$

Here, the shear stress S'u due to friction on the slope is given by

$$S'_u = \frac{\mu\gamma_t H_o x_o \cos\alpha}{h / \sin\alpha} \quad [7]$$

Introducing Eq. (7) into Eq. (6), one obtains

$$\Delta W = \frac{S_u}{4}(x_f^2 - x_o^2) + S'_u(\frac{h}{\sin\alpha})^2 \quad [8]$$

4.4 Equality of energy gain and energy loss

By equating the energy gain ΔE and energy loss ΔW, it is possible to derive a formula to back-estimate the residual strength S_u and S'_u. In doing so, two cases will be considered separately as follows.

4.5 Case 1

The residual strength mobilized during the sliding may be postulated to be equal to that at the time of the spreading. By putting Su=S'u in Eq. (8), and by putting ΔE=ΔW from Eqs. (5) and (8), an equality of energy is obtained. From the equality condition, the formula to back-estimate the residual strength can be obtained as

$$S_u = \frac{4\gamma_t H_o x_o (h - \frac{x_o}{2}\sin\alpha + \frac{H_o}{2}\cos\alpha - \frac{3}{8}H_f)}{(x_f^2 - x_o^2) + 4(\frac{h}{\sin\alpha})^2} \quad [9]$$

It is to be noticed that, if the variable Hf is quoted from Eq. (3), Eq. (9) is regarded as a third order algebraic equation with respect to the variable xf. Thus, if the residual strength Su is known by some means, it becomes possible to estimate the runout distance, xf, of the debris involved in a landslide.

4.6 Case 2

When the movement of a sliding mass is fast, the friction at the base of the slope would be negligibly small,

and the resistance on the slope may be disregarded. By putting $S'_u = 0$ in Eq. (8), the equality equation of energy, $\Delta E = \Delta W$ leads to the formula to back-estimate the residual strength as follows,

$$S_u = \frac{4\gamma_t H_o x_o (h - \frac{x_o}{2}\sin\alpha + \frac{H_o}{2}\cos\alpha - \frac{3}{8}H_f)}{(x_f^2 - x_o^2)} \quad [10]$$

In this case as well, Eq. (10) is deemed, with reference to Eq. (3), as a third order algebraic equation with respect to x_f to determine the runout distance of the landslide debris, if the value of S_u is known.

5. Interpretation of the residual strength from case studies and laboratory test

For the landslide in Tsukidate, the depth, H_0 and length x_0 of the soil mass involved in the slide are approximately known. The runout distance x_f and thickness H_f of the debris having spread over the rice field are known as well. Then, by using the formulae in Eqs. (9) And (10), it is possible to back-calculate the value of the residual strength Su. The data relevant to the flow movement at Tsukidate are as follows,

$H_0 = 5.4$m, $x_0 = 51$m, $\gamma_t = 14.3$tonf/m^3,

$\alpha = 11°$, $x_2 = 56.5$m, $h = 12.7$m & $x_f = 100$m

Introducing the above data into Eqs. (9) and (10), one can estimate the residual strength as Su =5kPa for the case 1 in which equal resistance is assumed for the sliding and spreading, and as being Su=11kPa for the case 2 where the resistance for the sliding phase is neglected. In interpreting these results, it is to be reminded that the energy loss in the course of sliding might be smaller than that spent during the process of spreading. Thus, the value of residual strength would probably lie between Su = 5 and 11kPa. However, in view of the fact that the residual strength as estimated above tends to overestimate the value of Su, the actual residual strength would be likely to be smaller than $S_u = 11$kPa. Apart from the arguments as above the value of $S_u = 5$ and 11kPa is plotted in **Fig. 27** superimposed to the residual strength determined from the laboratory tests. It is not known how much the water content was at the time the landslide occurred. However, judging from the presence of spring water on the exposed surface after the slide, it could as well be mentioned that the soil had been nearly saturated with the saturation ratio in excess of 60% and water content on the order of 30 to 50%. With these facts in mind, it may be mentioned that the laboratory-determined value of residual strength based on the constant volume change tests is well in the range of the value estimated by the back-analysis.

6. Conclusions

In an order clarify the mechanism of post-earthquake runout distance of landslide debris, the residual strength of soils mobilized at a largely deformed state is a factor of uttermost importance. In view of the fact that the soils involved in landslides are generally non-saturated, and also considering the rapidness in sliding masses, a new method which may be referred to as “constant volume triaxial test” was explored in this study to know the residual strength of partly saturated soils. The silty sand material secured from a site of earthquake-induced landslide was tested employing the above new test procedure. The outcome of the tests disclosed that, among several factors, the water content or saturation ratio is a key parameter governing the residual strength at a largely deformed state of the soil.

On the other hand, a back-analysis was performed, based on a simple kinematic model, for the known configuration of the landslide mass after it slid and spread out downhill. The value of the residual strength back-estimated from this analysis showed a reasonable level of coincidence with the value determined from the constant volume triaxial tests, provided proper assessment is made of the range of water content expected to have been prevailing in the silty sand around the slip surface.

Acknowledgements

The author wishes to express his sincere thanks to Professor Tsukamoto and former student Masanori Nakamura of Tokyo University of Science for their great efforts in conducting the laboratory tests and making analyses.

References

Hunter, G. & Fell, R., 2003. Travel Distance Angle for Rapid Landslides in Constructed and Natural Soil Slopes, Canadian Geotechnical Journal, **40**: 1123 - 1141.

Hungr, O., 1995. A Model for the Runout Analysis of Rapid Flow Slides, Debris Flows, and avalanches, Canadian Geotechnical Journal, **32**: 610-623.

Japanese Geotechnical Society, 2003. Report of Damage Investigation on Sanriku-Minami Earthquake and

Miyagiken-Hokubu Earthquake of 2003, Japanese Geotechnical Society.

Jeyapalan, J.K., 1982 Analyses of Earthquake-Induced Flow Slide Movements, *Proc. Soil Dynamics and Earthquake Engineering Conference*: 859-872. Southampton: UK.

Jeyapalan, J.K., 1983. Effects of Fluid Resistance in the Mine Waste Dam-Break Problem, *International Journal for Numerical and Analytical Methods in Geomechanics*, 7: 87-100.

Yasuda, S., Morimoto, I., Kiku, H. and Tanaka T. 2004. Reconnaissance Report on the Damage Causes by Three Japanese Earthquakes in 2003, *Proc. 3rd International Conference on Earthquake Geotechnical Engineering*, Berkeley: USA, 1: 14-21.